© Universiti Tun Hussein Onn Malaysia Publisher's Office

IJIE

http://penerbit.uthm.edu.my/ojs/index.php/ijie
ISSN : 2229-838X e-ISSN : 2600-7916

The International Journal of Integrated Engineering

A Fiber Bragg Grating-Based Gap Elongation Sensor for The Detection of Gap Elongation in Bolted Flange Connection

M.S.N.A. Adhreena[1], Z.M. Hafizi[1*], E. Vorathin[2]

[1]Advanced Structural Integrity and Vibration Research (ASIVR), Faculty of Mechanical and Automotive Engineering Technology, Universiti Malaysia Pahang, 26600 Pekan, Pahang Darul Makmur, MALAYSIA

[2]Department of Mechanical Engineering,
Universiti Teknologi PETRONAS, 32610 Seri Iskandar, Perak Darul Ridzuan, MALAYSIA

DOI: https://doi.org/10.30880/ijie.2022.14.08.010
Received 30 May 2022; Accepted 28 November 2022; Available online 21 December 2022

Abstract: Many attempts have been made by embedding a strain gauge sensor into the bolt shank to directly monitor the looseness of bolted structures. This application is constrained by many factors, including massive cabling connection, shortcomings of this sensor in harsh conditions, and low efficiency for high temperature applications. Therefore, fiber Bragg grating (FBG) sensing technology is a good alternative to solve the problem. In this article, an FBG-based gap elongation sensor was developed by embedding the sensor into a Teflon tube and clamping on the metal base structure. Several tests were carried out to calibrate the strain-sensitive coefficient of the sensor and also to determine the stability, linearity, and repeatability of the sensor for gap strain measurement. The strain sensitivity of the sensor was determined by a standard tensile test, with the strain sensitivity values ranging from 0.4221 pm/με to 0.5245 pm/με. During the calibration test, the FBG sensors showed excellent linearity and repeatability of less than 0.1% and 5% errors, respectively. The experimental results demonstrated a linear relationship between the applied force and the FBG sensor wavelength. Furthermore, the experimental results demonstrated acceptable linearity and stability of the sensor when subjected to bending loads with overall repeatability errors of less than 10%. This proposed method provides an alternative approach to monitor bolted gap elongation and characterize bolt looseness.

Keywords: Fiber Bragg grating, bolted flange joint, flange leak, gap opening

1. Introduction

A medium-sized refinery or oil and gas facility will typically contain approximately 50,000 to 100,000 bolted joint connections, in which all the joints have the potential to leak and create a risk to the plant and the environment, leading to catastrophic loss of life [1]. These production plants contain many chemical substances or hydrocarbons under pressure. Leakage in a process can cause a fire or an explosion, such as the incident of Piper Alpha [2, 3]. Several factors can induce and accelerate bolt loosening, with external load being the most crucial factor [4]. These bolted joints may be subjected to the torsional, axial tensile and bending external loads during the service. Their resistance to external loads is critical for the dynamic strength and also the reliability of the system. Therefore, an accurate and reliable inspection routine should be conducted frequently to monitor the structural integrity of these bolted connections [5, 6].

A monitoring system based on a fiber Bragg grating (FBG) sensor for structural health monitoring (SHM) has received wide attention due to its superior advantages. Its abilities to multiplex, immunity toward interferences, and withstand harsh environments make this sensor to be commercially developed as a smart system for structural monitoring. In general, FBG sensors use light as their signal carrier, which renders them immune to electromagnetic and electrostatic sources [7, 8]. Over the years, FBG sensors have been successfully embedded inside the bolt shank for

*Corresponding author: hafizi@ump.edu.my

monitoring the clamping force of bolted joints. Pran et al. conducted a long-term test to monitor creep in bolted glass-reinforced composite by embedding the FBG sensor at the center of the bolt [9]. The test proved that FBG sensors are applicable to field monitoring, but adhesive contributions should be considered. Ren et al. proposed a smart bolt concept that utilized four embedded FBG sensors to directly measure the axial and shear forces [10]. Later, Duan et al. analyzed the previous method and proposed self-temperature compensated FBG smart bolts for more practical application conditions [11]. However, embedding the sensor permanently into the host structure is commercially unappealing for SHM practices.

To address the shortcomings of smart bolt applications, an alternative approach for detecting bolt looseness was proposed in this study based on the gap elongation of the bolted flange connection by attaching the FBG sensor onto the clamping base structure. The experiment was conducted to acquire a linear relationship between the force applied on the flange joints and the central wavelength change of the FBG sensor. Furthermore, corresponding tests were performed to demonstrate the linearity and repeatability of the sensor design.

2. Working Principle of FBG Sensor

Strain predominates as the key parameter of interest in most engineering applications. For strain-sensing measurement, an applied load is directly transmitted from the host material to a particular location of fiber grating region by shear forces. This process will result in changes in grating length and cause the refractive index of the fiber core to vary over time. When the light source illuminates the FBG sensor and passes through the grating fringe, only a small portion of the light signal will be reflected back, while the remainder will pass through the sensor [12, 13]. This resulting a missing in a transmission signal. Fig. 1 shows a schematic diagram of the FBG working concept. The reflected signal is called Bragg wavelength, λ_B and any changes of the physical parameters at the grating section would affect the effective refractive index, η_{eff} and the spatial grating period, Λ at the core section of the sensor, as presented in Equation 1 [14]:

$$\lambda_B = 2\eta_{eff}\Lambda \tag{1}$$

When the strain, temperature, or other physical characteristics of the FBG environment change, the optical grating's refractive index would vary and thus affect the changes in the wavelength of reflected light. The following equation reflects the changes in FBG central wavelength, which is affected by strain and temperature:

$$\Delta\lambda_B = 2\left[\Lambda\frac{\partial\eta_{eff}}{\partial L} + \eta_{eff}\frac{\partial\Lambda}{\partial L}\right]\Delta L + 2\left[\Lambda\frac{\partial\eta_{eff}}{\partial T} + \eta_{eff}\frac{\partial\Lambda}{\partial T}\right]\Delta T \tag{2}$$

Based on Equation 2, the influence of strain effect is represented in the first term. The effect of compression and expansion will correspondingly change the effective index of the fiber, η_{eff}. When the FBG sensor is subjected to any changes in strain, and by neglecting temperature variance ($\Delta T = 0$), the shift in the Bragg wavelength can be expressed as:

$$\frac{\Delta\lambda_B}{\lambda_B} = (1-\rho_e)\varepsilon \tag{3}$$

where ρ_e is an effective photoelastic coefficient, with the value of germanium-doped silica fiber of 0.22, and ε is the axial strain of the grating.

3. Methodology

3.1 Fabrication of FBG-Based Gap Sensor

In this experiment, four FBG sensors were used to measure the shift in the Bragg wavelength. Sensors with different wavelengths of 1,540 nm, 1,545 nm, 1,548 nm, and 1,551 nm were adopted to evaluate the measurement of different bolt orientations of flange connection. To secure the bare fiber of the sensor, all FBG sensors were inserted into a hollow and transparent Teflon tube with an outer and inner diameter of 1 mm and 0.6 mm, respectively, as depicted in Fig. 4. The length of the Teflon tube is 50 mm. The grating of the FBG sensor was arranged on the central part of the tube. Then, the tube was filled with a cyanoacrylate adhesive using a syringe.

3.2 Strain Sensitivity Calibration of FBG-Based Gap Sensor

Before being applied to the flange joints, the strain-sensing behaviors of the FBG sensors must be characterized to determine their sensitivity coefficient. Fig. 2 illustrates the experimental setup for the sensitivity calibration of the

sensor. The embedded FBG sensor inside a Teflon tube was installed and clamped on the universal tensile testing machine, where the static load was constantly applied to the specimen with a machine speed of 0.1 mm/min. An FBG interrogator was set up to detect the shift of FBG central wavelength. During the experiment, the tensile machine was controlled to apply load with deformation in the range of 0-165 µm with an interval of 15 µm. The test signals monitored by the FBG interrogator were collected at each step. As the overall test time was relatively short, the room temperature may be considered as constant. The experiment was repeated three times for each sensor to evaluate its repeatability.

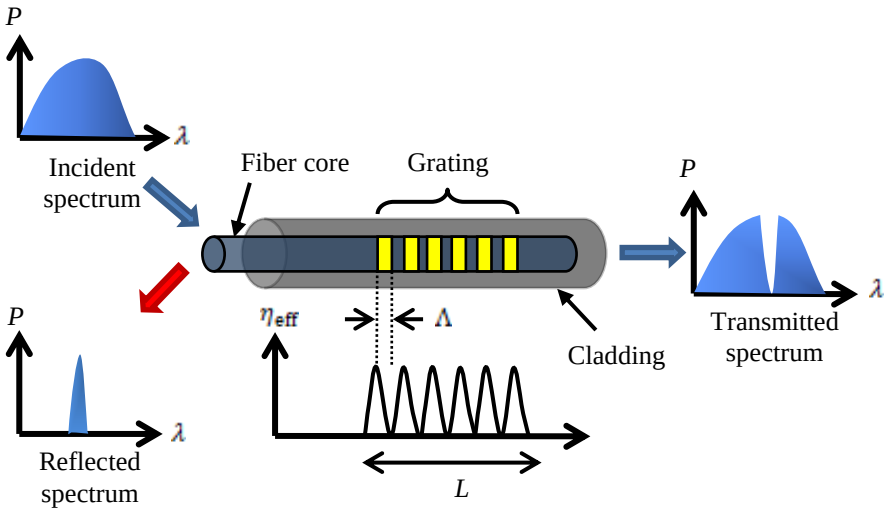

Fig. 1 - Schematic illustration of FBG sensor working principle

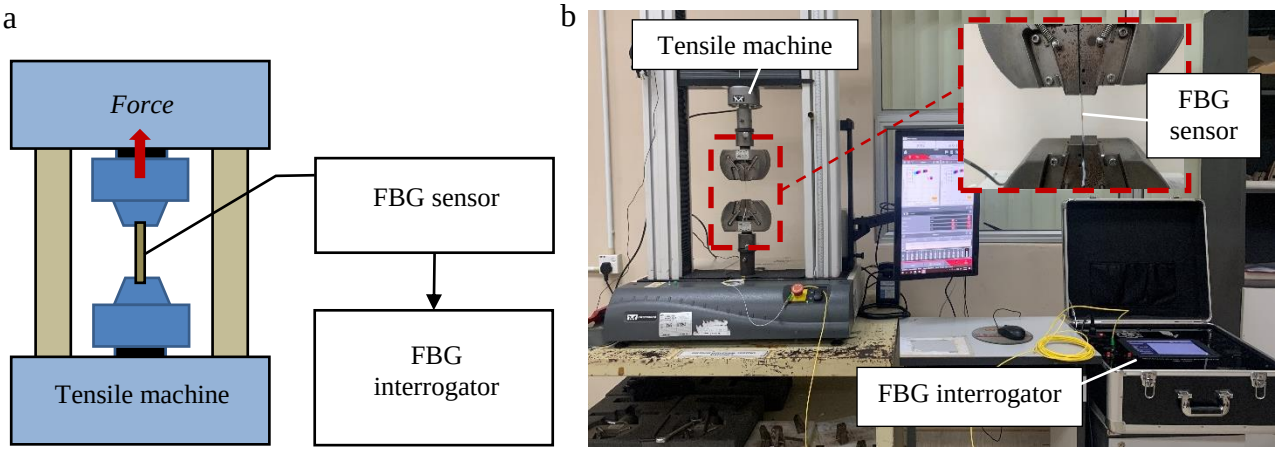

Fig. 2 - Experimental setup (a) schematic diagram and; (b) actual image

The experimental strain behavior results of the FBG sensor with a central wavelength of 1,540 nm are presented in Fig. 3. From the respective graph, the strain-sensitive coefficient of the sensor can be directly determined. In Fig. 3(a), the FBG central wavelength shifted from a lower wavelength to a higher wavelength when the tensile load was applied. It can be observed that the linearity of strain measurement is very high, with a linear correlation coefficient of 0.9998. This indicates that the sensor exhibits excellent linearity with a percentage error of only 0.03%. The strain-sensitive coefficient of the sensor can be determined by the slope of the changes in FBG central wavelength against the changes of strain. From the graph in Fig. 3(a), the strain sensitivity of the sensor for 1,540 nm was measured at 0.4764 pm/με.

The experiments were repeated three times for each sensor to obtain more reliable results. The average values of strain coefficient can be determined, and the reliability of the sensor can be observed throughout the tests. Fig. 3(b) indicates that the data from the FBG sensor are consistent between the tests. Therefore, the reliability and repeatability of the proposed FBG-based strain sensor can be verified. The summary of the results for each sensor is tabulated in Table 1.

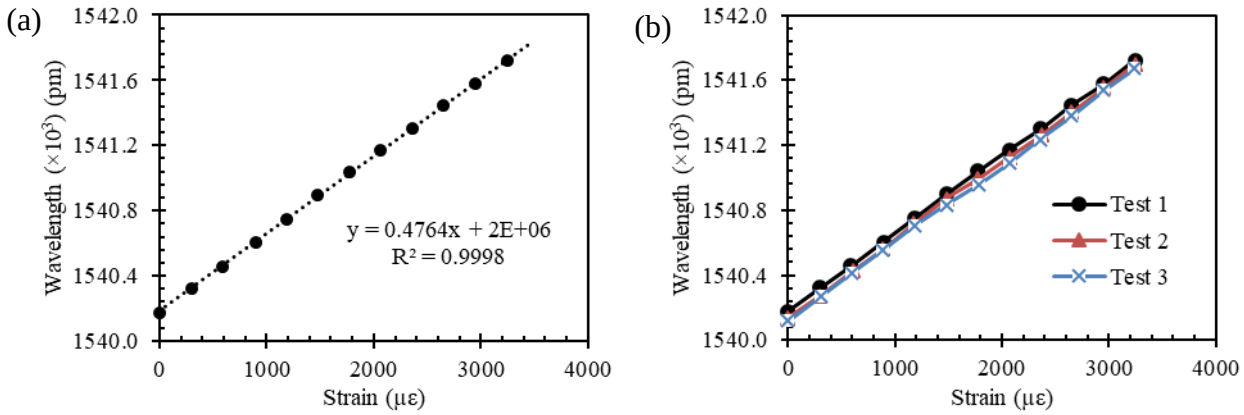

Fig. 3 - Experimental results of 1,540 nm (a) linearity graph and; (b) repeatability graph

Table 1 - Summary of experimental testing for each FBG sensor

FBG Central Wavelength	Average of Strain Sensitivity Coefficient (pm/με)	Average of Linear Correlation (R^2)	Linearity Error	Repeatability Error
1,540 nm	0.4767	0.9997	0.03%	0.96%
1,545 nm	0.5245	0.9993	0.07%	4.73%
1,548 nm	0.5130	0.9995	0.05%	3.76%
1,551 nm	0.4221	0.9997	0.03%	3.59%

From the results, all FBG sensors showed excellent linearity and repeatability with a small percentage error of less than 0.1% and 5% for linearity and repeatability, respectively. Overall, the FBG sensor appears to be more stable than a conventional strain gauge sensor. More details on the comparison between both sensors have been described in a separate study [15]. According to [15], the FBG sensor possesses much better data output in terms of linearity, stability, and repeatability, thus indicating that the FBG sensor can be recognized as realistic sensor instrumentation for structural monitoring.

3.3 Experimental Setup and FBG Interrogator

For bolted flange application, the FBG-based gap sensors consisted of a clamping structure. The structure includes top and bottom clamps fabricated using similar stainless steel material. Next, the FBG sensor encapsulated inside a Teflon tube was attached between the clamps, as illustrated in Fig. 4. The tube was then screwed on the top clamp to fix and lock its position.

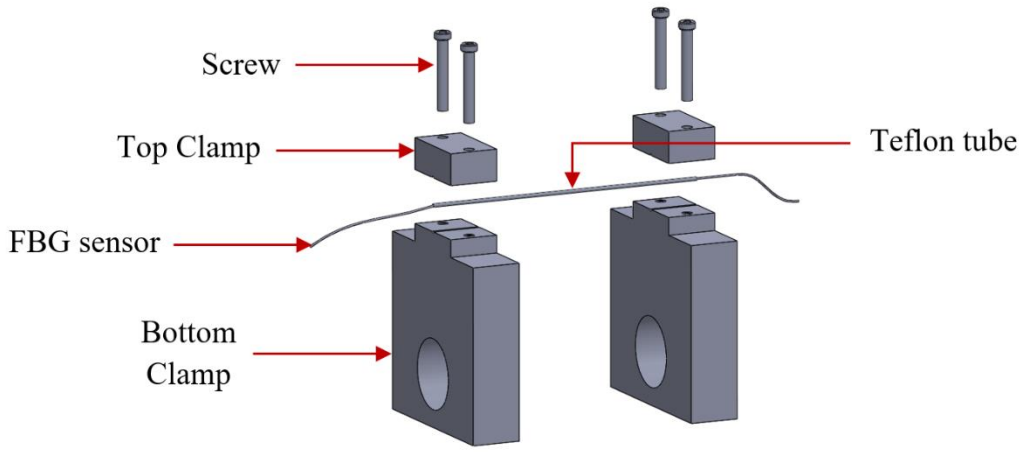

Fig. 4 - Three-dimensional model of FBG-based gap sensor

In this experiment, a C-channel steel structure was designed to support two 0.6-m long pipes, where each pipe was welded to an ANSI B16.5 steel flange on both ends. Four gap sensors were installed and distributed evenly on all four

bolted joints of the flange structure. For convenience, the four bolts are denoted as B1, B2, B3, and B4, as illustrated in Fig. 5(a). The bolt hole was symmetrical, and the axis was rotated up to 15° to analyze the gap elongation measurements at different bolt positions. It is crucial to control the stress variation in the bolted flanged joint components to secure a flange joint. Thus, all the bolts were tightened with a crisscross tightening pattern to avoid flange misalignment and minimize any possible faults.

A hydraulic press machine was utilized to induce gap opening on the bolted connection by exerting the force on top of the bolted flange connection. A load cell was positioned between the hydraulic press cylinder and the bolted flange connection to calibrate the applied force, as shown in Fig. 5(b). This setup was used to detect and measure the strain between the flange gap when certain FBG sensors are subjected to tension while others are subjected to compression.

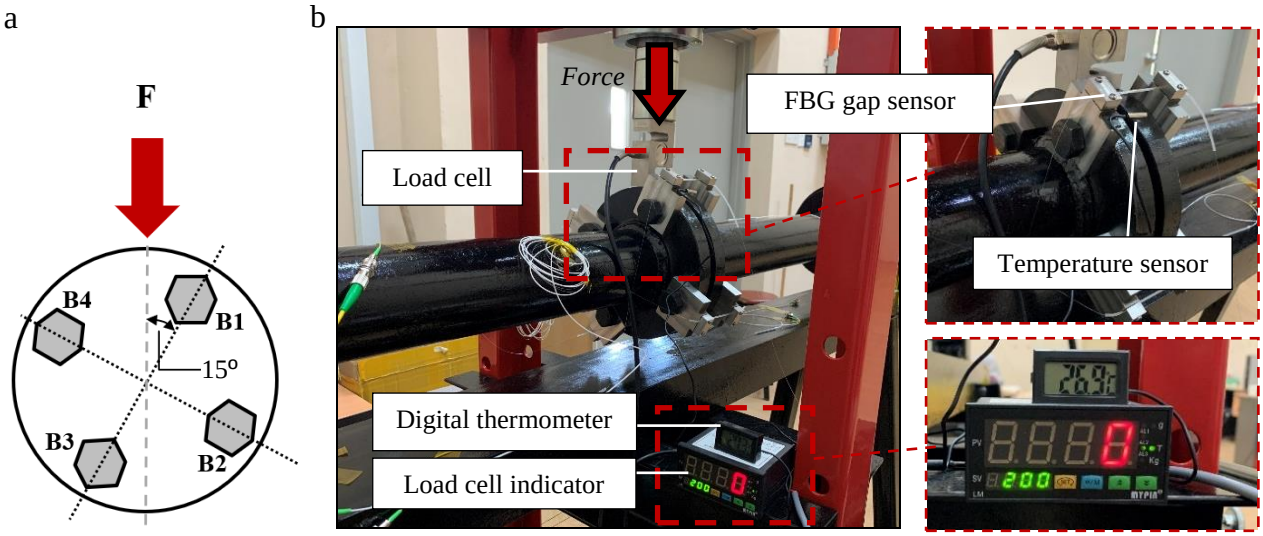

Fig. 5 - (a) Illustration of bolt layouts and; (b) experimental setup

The experiment was conducted at a controlled room temperature with temperature variances of ± 0.3 °C. A digital thermometer was employed, and its probe was located near the FBG sensor to monitor the surrounding temperature. At a controlled room temperature of 26.9 °C, the relationship between the shift of FBG central wavelength and the strain parameter can be expressed as Equation 3 [16]. Each sensor was installed and set with a pre-strained value to measure the positive and negative strains of the FBG sensors. Table 2 lists the bolt positions and their corresponding FBG wavelengths before (original wavelength) and after installation (pre-strained wavelength).

Table 2 - FBG wavelength before and after installation

Bolt position	FBG Wavelength (Before Installation)	FBG Wavelength (After Installation)
B1	1,540.016 nm	1,540.970 nm
B2	1,545.404 nm	1,546.174 nm
B3	1,548.226 nm	1,549.067 nm
B4	1,551.137 nm	1,551.883 nm

In the FBG interrogation setup, a super luminescent diode (SLD) light source with an output power of 600 mA was employed to monitor the FBG central wavelength. An optical circulator was then used to connect the SLD light source and FBG sensors. Four FBG sensors were multiplexed together to form a single line fiber, as illustrated in Fig. 6. A high-speed of FBG interrogator with a minimum resolution of 1 pm and 1,000 Hz sampling frequency was utilized to acquire the FBG wavelength data.

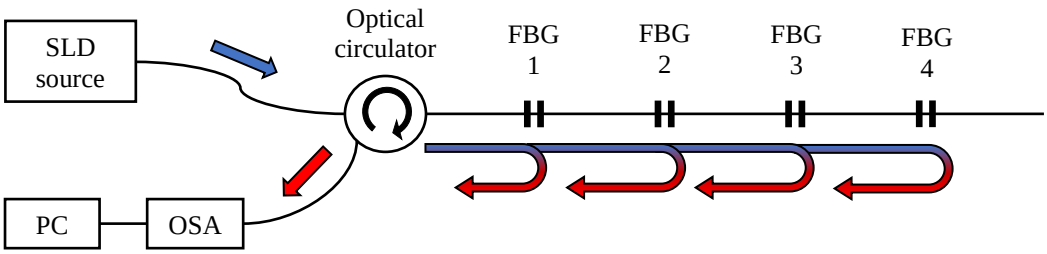

Fig. 6 - Schematic illustration of the FBG interrogation system

4. Results and Discussion

4.1 Wavelength Response of FBG Strain Sensor

To determine the strain response of the sensor, the force induced on top of the bolted flanged was varied from 0 to 2,000 N, with a step of 200 N. All the bolts were tightened with a fixed torque of 10 Nm. Fig. 7 presents the strain response of the FBG gap sensor versus the applied force to indicate the linearity of the sensor.

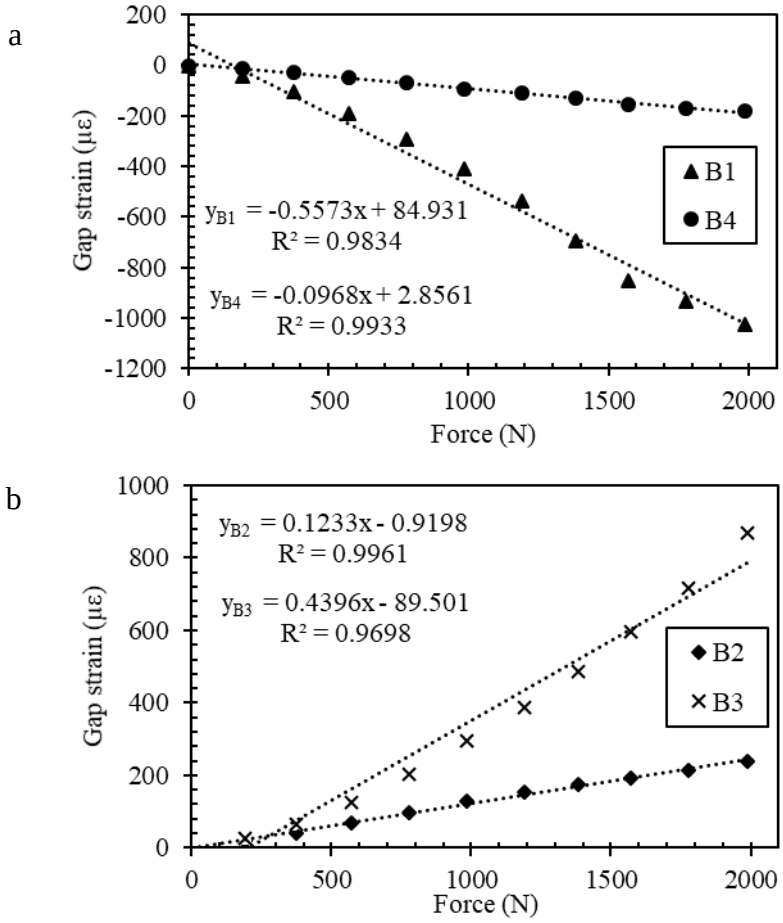

Fig. 7 - Linearity of the FBG strain response at (a) B1 and B4 and; (b) B2 and B3

From these graphs, all the sensors for B1, B2, B3, and B4 demonstrated almost linear correlation coefficients, which are 0.9834, 0.9961, 0.9698, and 0.9933, respectively. However, it can be observed that the sensors produced a different graph trend depending on their position. The sensors on B1 and B4 experienced negative strain values, whereas the sensors on B2 and B3 experienced positive strain values.

By comparing both negative strain measurements as in Fig. 7(a), the average center wavelength change for B1 was 5.8 times higher than B4, with the maximum strain values of -1,026.17 με for B1 and -177.50 με for B4. On the other hand, by comparing both positive strain measurements in Fig. 7(b), the average center wavelength change for B3 was 3.7 times higher than B2, with the maximum strain values of 869.67 με for B3 and 238.0 με for B2. It can be deduced that B1 experienced higher critical compression as the sensor was adjacent to the point of impact/load, while B3, which was directly opposite to the point of loading, experienced a critical tension state.

To test the repeatability of the sensor, the experiment was repeated three times with the loading and unloading conditions. The force was maintained for 5 min in each step to acquire much more stable data measurement. The test results for all sensors are shown in Fig. 8. The sensors' responses were consistent within the three cycles, with overall repeatability errors of less than 10%. However, the Bragg wavelength showed a slight discrepancy of approximately 20% error between loading and unloading conditions. This is because the sensors might suffer from hysteresis effects due to the use of a Teflon tube.

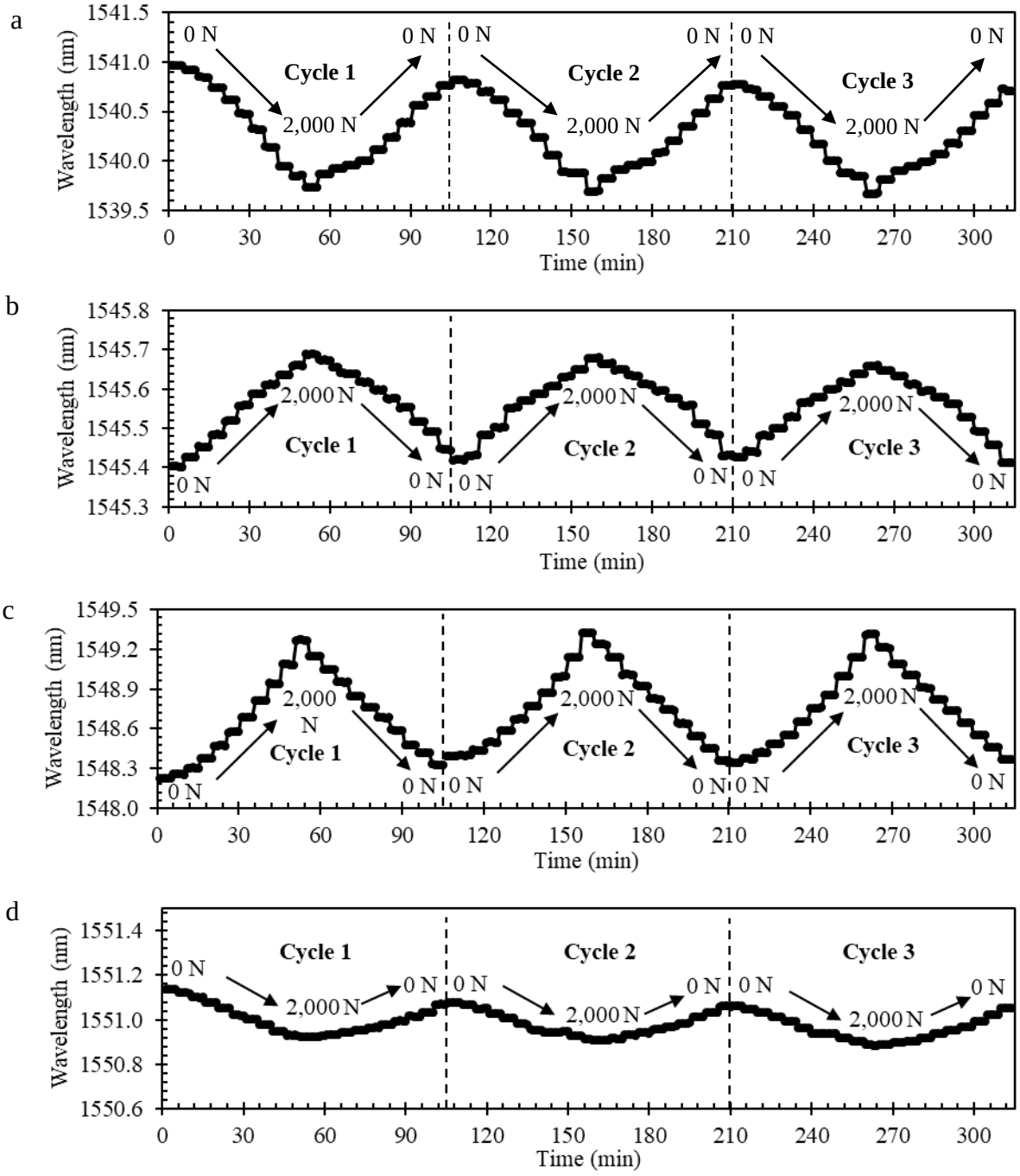

Fig. 8 - Repeatability response of the FBG gap sensors at (a) B1; (b) B2; (c) B3, and; (d) B4

4.2 The Effect of Torque Variation

To investigate the relationship between the applied torque and the gap strain, the experiment was repeated by increasing the bolt torque to 20 Nm. All the bolts were manually tightened using a torque wrench. Fig. 9 was plotted by comparing both graph patterns for 10 Nm and 20 Nm torque values.

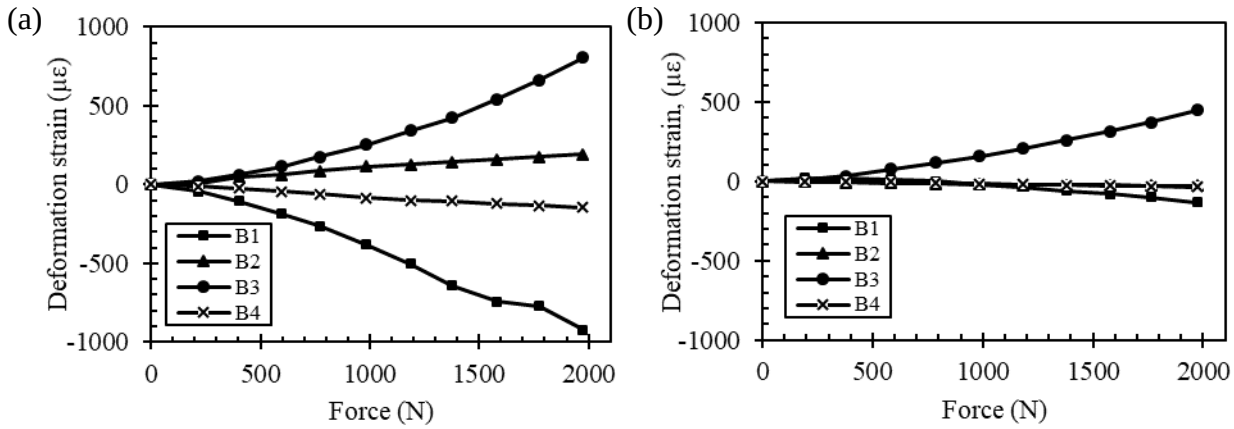

Fig. 9 - The strain gap variations of the FBG gap sensor during the test at the torque values of (a) 10 Nm and; (b) 20 Nm

In Fig. 9(b), the strain decreased significantly when the bolts were tightened at 20 Nm. At the maximum of 2,000 N, the strain at critical points B1 and B3 dropped significantly by 87% and 48.5%, respectively. Meanwhile, the strain at B2 and B4 decreased by 88.8% and 80%, respectively. This may deduce that lower torque will increase the gap strain on the bolted joints and vice versa. Overall, the FBG gap sensor can characterize the loosening process quantitatively.

5. Conclusion

This paper developed a practical technique for monitoring the strain gap on the bolted flange using the FBG sensor. An effective test setup was designed and fabricated to verify the performance of the FBG gap sensor. With all the merits of optical fibers, the proposed sensor can precisely measure the gap strain on a bolted flange connection with the strain sensitivity of 0.4221-0.5245 pm/με. The experimental results demonstrated a linear relationship between the applied force and the central wavelength of the FBG gap sensor. The response of the gap sensor was consistent within the test with errors less than 10%. However, the sensors experienced hysteresis effects, which might be due to soft sealing materials, such as Teflon tube. Overall, the FBG gap sensors possess good accuracy, stability, and repeatability for the gap strain measurement of the bolted flange. The sensors can also characterize the torque variation, where the gap strain reduced up to 80% when the nuts were tightened from 10 Nm to 20 Nm. Therefore, it can be justified that the gap strain decreases as the bolts are tightened with higher torque.

Acknowledgement

The authors would like to acknowledge UMP Research and Innovation Department for providing the UMP Internal Research Grant (RDU1903120); the Ministry of Higher Education for providing financial support under Fundamental Research Grant Scheme (FRGS), FRGS/1/2019/TK03/UMP/02/7 (University reference RDU1901116); and Postgraduate Research Grants Scheme (PGRS) under grant no. PGRS2003145. The authors would also like to acknowledge the Faculty of Mechanical & Automotive Engineering Technology, Universiti Malaysia Pahang (http://www.ump.edu.my/) for providing the laboratory facilities. Finally, special thanks to the Institute of Postgraduate Studies (IPS), Universiti Malaysia Pahang for funding through the Master Research Scheme (MRS) scholarship.

References

[1] Jaszak, P., & Adamek, K. (2019) Design and analysis of the flange-bolted joint with respect to required tightness and strength. Open Engineering, 9, 338-49.

[2] Paté-Cornell, M. E. (1993). Learning from the Piper Alpha accident: A postmortem analysis of technical and organizational factors. Risk Analysis, 13, 215-32.

[3] Preventor, J. E. & Proactima, W. R. (2013). Norwegian oil and gas industry project to reduce the number of hydrocarbon leaks with emphasis on operational barriers improvement. In: European HSE Conference and Exhibition, (London, United Kingdom)

[4] Noda N-A., Chen, X., Sano, Y., Wahab, M. A., Maruyama, H., Fujisawa, R., & Takase, Y. (2016) Effect of pitch difference between the bolt-nut connections upon the anti-loosening performance and fatigue life. Materials & Design, 96, 476-89.

[5] Ho, S., Li, W., Wang, B., & Song, G. (2017). A load measuring anchor plate for rock bolt using fiber optic sensor. Smart Materials and Structures, 26, 057003.

[6] Jung, B. H., Kim, Y. W., & Lee, J. R. (2019). Laser-based structural training algorithm for acoustic emission localization and damage accumulation visualization in a bolt joint structure. Structural Health Monitoring, 18, 1851-61.
[7] Meribout, M., & Khezzar, L. (2020). Leak detection systems in oil and gas fields: Present trends and future prospects. Flow Measurement and Instrumentation, 75, 101772.
[8] Vorathin, E., Hafizi, Z., Ismail, N., Loman, M., Aizzuddin, A., Lim, K. S., & Ahmad, H. (2019). FBG water-level transducer based on PVC-cantilever and rubber-diaphragm structure. IEEE Sensors Journal, 19, 7407-14.
[9] Pran, K., Farsund, O., & Wang, G. (2002). Fibre Bragg grating smart bolt monitoring creep in bolted GRP composite. In: 2002 15th Optical Fiber Sensors Conference Technical Digest, (Oregon, United States: IEEE) 431-434.
[10] Ren, L., Feng, T., Ho, M., Jiang, T., & Song, G. (2018). A smart "shear sensing" bolt based on FBG sensors. Measurement, 122, 240-6.
[11] Duan, C., Zhang, H., Li, Z., Tian, Y., Chai, Q., Yang, J., et al. (2020). FBG smart bolts and their application in power grids. IEEE Transactions on Instrumentation and Measurement, 69, 2515-2521.
[12] Luyckx, G., Voet, E., Lammens, N., & Degrieck, J. (2011). Strain measurements of composite laminates with embedded fibre Bragg gratings: Criticism and opportunities for research. Sensors, 11, 384-408.
[13] Lau, K. T., Zhou, L., & Wu, J. (2001). Investigation on strengthening and strain sensing techniques for concrete structures using FRP composites and FBG sensors. Materials and Structures, 34, 42-50.
[14] Ma, Z., & Chen, X. (2020). Strain transfer characteristics of surface-attached FBGs in aircraft wing distributed deformation measurement. Optik, 207, 164468.
[15] Shukri, N. A. A. M., Zohari, M. H., & Epin, V. (2021). Surface strain measurement on pressurized thick-walled pipe by fiber Bragg grating sensor and strain gauges. Journal of Advanced Research in Fluid Mechanics and Thermal Sciences, 84, 1-9.
[16] Vorathin, E., & Hafizi, Z. M. (2020). Bandwidth modulation and centre wavelength shift of a single FBG for simultaneous water level and temperature sensing. Measurement, 163, 107955.